Electronic Supplementary Material (ESI) for Journal of Materials Chemistry C.

supporting information

Ligand Field Fine-tuning on Modulation of Magnetic Properties and Relaxation Dynamics for Dysprosium (III) Single-Ion Magnets (SIMs): Synthesis, Structure, Magnetism and *Ab Initio* Calculations

Sheng Zhang, [a,b] Haipeng Wu, [a] Lin Sun, [a] Hongshan Ke, [a] Sanping Chen,*[a] Bing Yin,*[a] Qing Wei, [a] Desuo Yang, [b] Shengli Gao[a]

[a] Prof. Sanping. Chen, Dr. B. Yin

Key Laboratory of Synthetic and Natural Functional Molecule Chemistry of Ministry of Education, College of Chemistry and Materials Science, Northwest University, Xi'an, Shaanxi 710069, China.

[b] Dr. Sheng Zhang, Prof. Desuo Yang

College of Chemistry and Chemical Engineering, Baoji University of Arts and Sciences, Baoji 721013, China.

Corresponding authors

Prof. Sanping Chen

E-mail address: sanpingchen@126.com

Prof. Bing Yin

E-mail address: rayinyin@nwu.edu.cn

Table S1. Crystallographic Data for the compounds **1-4.**

Compound	**1**	**2**	**3**	**4**
Empirical formula	$C_{41.33}H_{25.67}DyF_{12}$ $N_2O_{6.33}$	$C_{42}H_{23}Dy$ $F_{12}N_2O_6$	$C_{43}H_{32}Dy$ $F_9N_2O_6$	$C_{45}H_{36}Dy$ $F_9N_2O_7$
Formula weight	1042.14	1042.12	1006.21	1050.26
Temperature	296(2) K	296(2) K	293(2)	296(2) K
Crystal system	Trigonal	Triclinic	Triclinic	Triclinic
space group	*P*-3	*P*-1	*P*-1	*P*-1
a (Å)	26.791(4)	10.273(2)	12.429(3)	10.8160(11)
b (Å)	26.791(4)	13.625(3)	17.651(4)	10.9937(11)
c (Å)	10.119(2)	15.204(3)	21.655(5)	18.5997(18)
α (°)	90	83.405(4)	87.902(5)	81.692(2)
β (°)	90	87.777(4)	74.279(5)	86.565(2)
γ (°)	120	76.586(4)	71.393(4)	84.476(2)
V (Å^3)	6289.8(19)	2056.1(7)	4327.5(18)	2166.2(4)
Z	6	2	2	2
F(000)	3074	1022	1996	1046
Goodness of fit (F^2)	1.022	1.051	1.099	1.082
Final *R* indices [I>2sigma(I)]	$R1 = 0.0652$ $wR_2 = 0.1243$	$R1 = 0.0637$ $wR_2 = 0.1391$	$R1 = 0.1032$ $wR_2 = 0.2068$	$R1 = 0.0359$ $wR_2 = 0.1052$
R indices (all data)	$R1 = 0.1382$ $wR_2 = 0.1415$	$R1 = 0.1739$ $wR_2 = 0.1905$	$R1 = 0.1225$ $wR_2 = 0.2561$	$R1 = 0.0400$ $wR_2 = 0.1150$
CCDC	1446105	1445984	1518734	1518732

Table S2. Selected bond lengths (Å) and angles (°) for **1-4.**

1					
Dy(1)-O(1)	2.290(7)	O(1)-Dy(1)-O(5)	82.1(3)	O(1)-Dy(1)-O(3)	142.0(3)
Dy(1)-O(4)	2.295(7)	O(4)-Dy(1)-O(5)	75.0(2)	O(4)-Dy(1)-O(3)	73.1(3)
Dy(1)-O(2)	2.301(7)	O(2)-Dy(1)-O(5)	148.8(3)	O(2)-Dy(1)-O(3)	74.7(2)
Dy(1)-O(3)	2.326(7)	O(3)-Dy(1)-O(5)	118.2(3)	O(1)-Dy(1)-O(6)	143.1(3)
Dy(1)-O(6)	2.341(7)	O(6)-Dy(1)-O(5)	70.2(3)	O(4)-Dy(1)-O(6)	111.4(3)
Dy(1)-O(5)	2.381(8)	O(1)-Dy(1)-N(2)	111.0(3)	O(2)-Dy(1)-O(6)	139.8(2)
Dy(1)-N(2)	2.529(9)	O(4)-Dy(1)-N(2)	149.3(3)	O(1)-Dy(1)-N(1)	74.4(3)
Dy(1)-N(1)	2.558(8)	O(2)-Dy(1)-N(2)	75.7(3)	O(4)-Dy(1)-N(1)	146.9(3)
O(1)-Dy(1)-O(4)	83.1(3)	O(3)-Dy(1)-N(2)	80.0(3)	O(2)-Dy(1)-N(1)	112.3(2)
O(1)-Dy(1)-O(2)	73.3(3)	O(6)-Dy(1)-N(2)	74.2(3)	O(3)-Dy(1)-N(1)	138.0(3)
O(4)-Dy(1)-O(2)	83.0(3)	O(5)-Dy(1)-N(2)	132.4(3)	O(6)-Dy(1)-N(1)	76.4(3)

O(3)-Dy(1)-O(6)	74.4(2)	N(2)-Dy(1)-N(1)	63.4(3)	O(5)-Dy(1)-N(1)	78.2(3)
			2		
Dy(1)-O(3)	2.286(8)	O(3)-Dy(1)-O(1)	71.7(3)	O(3)-Dy(1)-O(5)	142.7(2)
Dy(1)-O(6)	2.302(9)	O(6)-Dy(1)-O(1)	138.8(3)	O(6)-Dy(1)-O(5)	72.6(2)
Dy(1)-O(2)	2.307(8)	O(2)-Dy(1)-O(1)	72.7(3)	O(2)-Dy(1)-O(5)	75.0(3)
Dy(1)-O(5)	2.311(8)	O(5)-Dy(1)-O(1)	142.6(3)	O(3)-Dy(1)-O(4)	71.5(3)
Dy(1)-O(4)	2.327(7)	O(4)-Dy(1)-O(1)	115.3(3)	O(6)-Dy(1)-O(4)	87.8(2)
Dy(1)-O(1)	2.334(10)	O(3)-Dy(1)-N(2)	138.0(3)	O(2)-Dy(1)-O(4)	81.7(3)
Dy(1)-N(2)	2.553(10)	O(6)-Dy(1)-N(2)	93.7(3)	O(5)-Dy(1)-O(4)	77.5(2)
Dy(1)-N(1)	2.605(9)	O(2)-Dy(1)-N(2)	81.3(3)	O(3)-Dy(1)-N(1)	76.0(4)
O(3)-Dy(1)-O(6)	85.7(3)	O(5)-Dy(1)-N(2)	74.9(3)	O(6)-Dy(1)-N(1)	71.2(3)
O(3)-Dy(1)-O(2)	119.2(3)	O(4)-Dy(1)-N(2)	150.5(4)	O(2)-Dy(1)-N(1)	131.9(3)
O(6)-Dy(1)-O(2)	147.4(3)	O(1)-Dy(1)-N(2)	82.1(3)	O(5)-Dy(1)-N(1)	122.2(3)
O(4)-Dy(1)-N(1)	142.3(4)	O(1)-Dy(1)-N(1)	70.2(3)	O(3)-Dy(1)-O(1)	71.7(3)

3

Dy(1)-O(2)	2.28(3)	O(6-Dy(1)-O(3)	139.5(9)
Dy(1)-O(6)	2.30(3)	O(6)-Dy(1)-N2)	72.7(9)
Dy(1)-O(5)	2.33(3)	O(5)-Dy(1)-N(1)	136.8(8)
Dy(1)-O(4)	2.34(3)	O(5)-Dy(1)-O(4)	77.3(10)
Dy(1)-O(3)	2.36(2)	O(5)-Dy(1)-O(3)	145.2(9)
Dy(1)-O(1)	2.28(2)	O(5)-Dy(1)-N(2)	80.7(9)
N(1)-Dy(1)-N2)	64.1(9)	O(4)-Dy(1)-N(1)	114.1(9)
O(2)-Dy(1)-N(1)	80.2(8)	O4)-Dy(1)-O(3)	71.3(9)
O(2)-Dy(1)-O(6)	79.5(9)	O(4)-Dy(1)-N(2)	75.2(9)
O(2)-Dy(1)-O(5)	119.3(10)	O(3)-Dy(1)-N(1)	72.0(8)
O(2)-Dy(1)-O(4)	139.5(9)	O(3)-Dy(1)-N(2)	104.9(9)
O(2)-Dy(1)-O(3)	78.6(9)	O(1)-Dy(1)-N(1)	145.9(8)
O(2)-Dy(1)-O(1)	73.6(8)	O(1)-Dy(1)-O(6)	123.5(9)
O(2)-Dy(1)-N(2)	140.1(9)	O(1)- Dy(1)-O(5)	76.4(9)
O(6)-Dy(1)-N(1)	71.0(9)	O(1)- Dy(1)-O(4)	75.7(9)
O(6)-Dy(1)-O(5)	75.3(10)	O1)- Dy(1)-O(3)	81.6(8)
O(6)-Dy(1)-O(4)	140.4(9)	O(1)- Dy(1)-N(2)	146.1(9)
N(1)-Dy(1)	2.477(18)	Dy(1)-N(2)	2.53(3)

4

Dy(1)-O(5)	2.307(3)	O(3)-Dy(1)-O(2)	75.07(12)
Dy(1)-O(6)	2.315(3)	O(5)-Dy(1)-O(4)	77.71(11)
Dy(1)-O(1)	2.319(3)	O(6)-Dy(1)-O(4)	141.62(11)
Dy(1)-O(3)	2.333(3)	O(1)-Dy(1)-O(4)	75.78(11)

Dy(1)-O(2)	2.336(3)	O(3)-Dy(1)-O(4)	71.75(11)
Dy(1)-O(4)	2.359(3)	O(2)-Dy(1)-O(4)	136.13(11)
Dy(1)-N(1)	2.544(4)	O(5)-Dy(1)-N(1)	134.04(11)
Dy(1)-N(2)	2.554(4)	O(6)-Dy(1)-N(1)	72.13(11)
O(5)-Dy(1)-O(6)	73.26(10)	O(1)-Dy(1)-N(1)	150.50(12)
O(5)-Dy(1)-O(1)	74.08(11)	O(3)-Dy(1)-N(1)	74.74(12)
O(6)-Dy(1)-O(1)	118.28(11)	O(2)-Dy(1)-N(1)	82.83(12)
O(5)-Dy(1)-O(3)	145.59(11)	O(4)-Dy(1)-N(1)	114.31(12)
O(6)-Dy(1)-O(3)	141.11(11)	O(5)-Dy(1)-N(2)	79.56(12)
O(1)-Dy(1)-O(3)	83.26(11)	O(6)-Dy(1)-N(2)	75.90(12)
O(5)-Dy(1)-O(2)	120.27(11)	O(1)-Dy(1)-N(2)	143.73(12)
O(6)-Dy(1)-O(2)	81.12(11)	O(3)-Dy(1)-N(2)	106.53(12)
O(1)-Dy(1)-O(2)	72.54(11)	O(2)-Dy(1)-N(2)	143.50(12)

Table S3. Dy^{III} ion geometry analysis of **1-4** by SHAPE 2.1 software.

Dy^{III} ion geometry analysis of **1**

```
HBPY-8          3 D6h   Hexagonal bipyramid
CU-8            4 Oh    Cube
SAPR-8          5 D4d   Square antiprism
TDD-8           6 D2d   Triangular dodecahedron
JGBF-8          7 D2d   Johnson gyrobifastigium J26
JETBPY-8        8 D3h   Johnson elongated triangular bipyramid J14
JBTPR-8         9 C2v   Biaugmented trigonal prism J50
BTPR-8         10 C2v   Biaugmented trigonal prism
JSD-8          11 D2d   Snub diphenoid J84

Structure [ML8 ]     HBPY-8      CU-8      SAPR-8      TDD-8      JGBF-8    JETBPY-8    JBTPR-8     BTPR-8      JSD-8
 ABOXIY       ,      16.036,     9.293,     0.511,     2.267,     15.933,    28.208,     2.818,      2.207,     5.166
```

Dy^{III} ion geometry analysis of **2**

```
HBPY-8          3 D6h   Hexagonal bipyramid
CU-8            4 Oh    Cube
SAPR-8          5 D4d   Square antiprism
TDD-8           6 D2d   Triangular dodecahedron
JGBF-8          7 D2d   Johnson gyrobifastigium J26
JETBPY-8        8 D3h   Johnson elongated triangular bipyramid J14
JBTPR-8         9 C2v   Biaugmented trigonal prism J50
BTPR-8         10 C2v   Biaugmented trigonal prism
JSD-8          11 D2d   Snub diphenoid J84

Structure [ML8 ]     HBPY-8      CU-8      SAPR-8      TDD-8      JGBF-8    JETBPY-8    JBTPR-8     BTPR-8      JSD-8
 ABOXIY       ,      15.550,    10.541,     1.344,     1.509,     14.497,    28.104,     1.785,      1.314,     4.070
```

Dy^{III} ion geometry analysis of **3**

```
-------------------------------------------------------------------------------
S H A P E   v2.1        Continuous Shape Measures calculation
(c) 2013  Electronic Structure Group, Universitat de Barcelona
                 Contact:  llunell@ub.edu
-------------------------------------------------------------------------------

PtL4 structures

HBPY-8          3 D6h   Hexagonal bipyramid
CU-8            4 Oh    Cube
SAPR-8          5 D4d   Square antiprism
TDD-8           6 D2d   Triangular dodecahedron
JGBF-8          7 D2d   Johnson gyrobifastigium J26
JETBPY-8        8 D3h   Johnson elongated triangular bipyramid J14
JBTPR-8         9 C2v   Biaugmented trigonal prism J50
BTPR-8         10 C2v   Biaugmented trigonal prism
JSD-8          11 D2d   Snub diphenoid J84

Structure [ML8 ]     HBPY-8      CU-8      SAPR-8      TDD-8      JGBF-8    JETBPY-8    JBTPR-8     BTPR-8
   JSD-8
 ABOXIY       ,      15.510,    10.186,     0.834,     2.300,     14.919,    27.555,     2.342,      1.730,
   4.886
```

Dy^{III} ion geometry analysis of **4**

```
-------------------------------------------------------------------------------
S H A P E   v2.1          Continuous Shape Measures calculation
(c) 2013  Electronic Structure Group, Universitat de Barcelona
                   Contact:  llunell@ub.edu
-------------------------------------------------------------------------------

PtL4 structures

HBPY-8          3 D6h    Hexagonal bipyramid
CU-8            4 Oh     Cube
SAPR-8          5 D4d    Square antiprism
TDD-8           6 D2d    Triangular dodecahedron
JGBF-8          7 D2d    Johnson gyrobifastigium J26
JETBPY-8        8 D3h    Johnson elongated triangular bipyramid J14
JBTPR-8         9 C2v    Biaugmented trigonal prism J50
BTPR-8         10 C2v    Biaugmented trigonal prism
JSD-8          11 D2d    Snub diphenoid J84

Structure [ML8 ]      HBPY-8        CU-8       SAPR-8        TDD-8       JGBF-8      JETBPY-8       JBTPR-8
BTPR-8        JSD-8
 ABOXIY         ,     16.139,       9.026,       0.557,       1.994,      16.464,      27.854,       2.664,
 2.135,        4.959
```

Configuration	ABOXIY, **1**	ABOXIY, **2**	ABOXIY, **3**	ABOXIY, **4**
Hexagonal bipyramid (D_{6h})	16.036	15.550	15.510	16.139
Cube (O_h)	9.293	10.541	10.186	9.026
Square antiprism (D_{4d})	0.511	1.344	0.834	0.557
Triangular dodecahedron (D_{2d})	2.267	1.509	2.300	1.994
Johnson gyrobifastigium J26 (D_{2d})	15.933	14.497	14.919	16.464
Johnson elongated triangular bipyramid J14 (D_{3h})	28.208	28.104	27.555	27.845
Biaugmented trigonal prism J50 (C_{2v})	2.818	1.785	2.342	2.664
Biaugmented trigonal prism (C_{2v})	2.207	1.314	1.730	2.135
Snub siphenoid J84 (D_{2d})	5.166	4.070	4.886	4.959

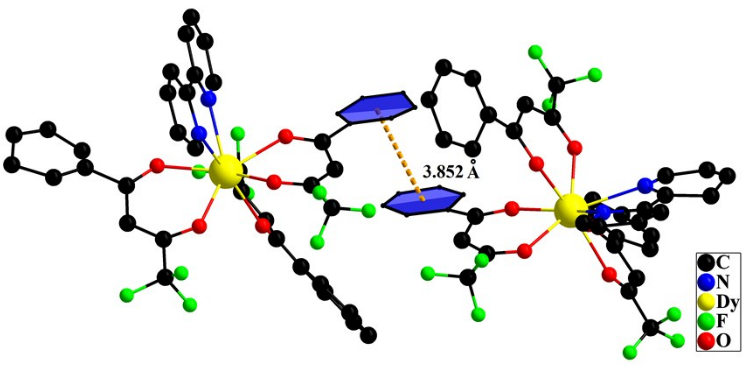

Figure S1. Packing arrangement between two neutral in **3**.

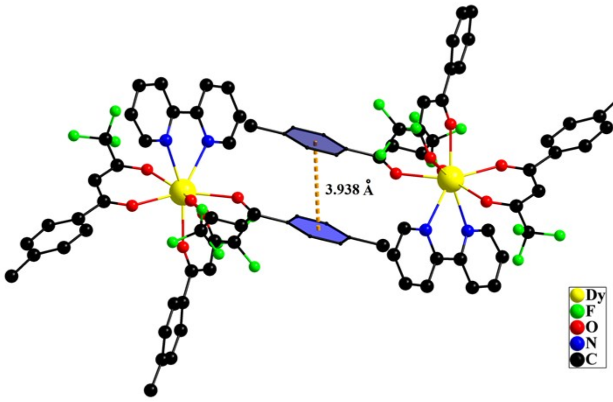

Figure S2. Packing arrangement between two neutral in **4**.

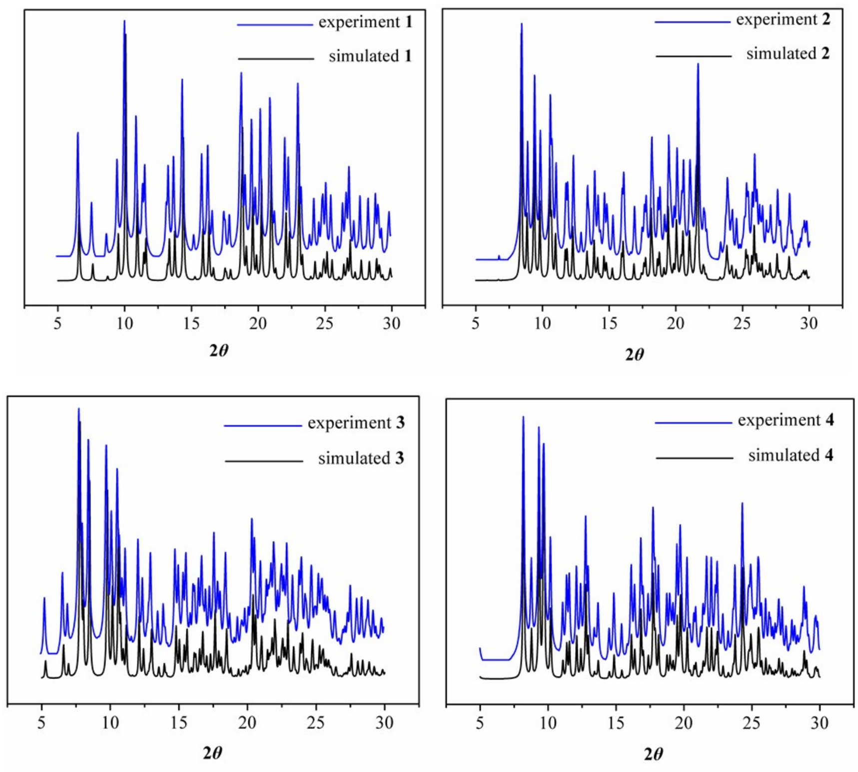

Figure S3. XRPD curves of **1-4.**

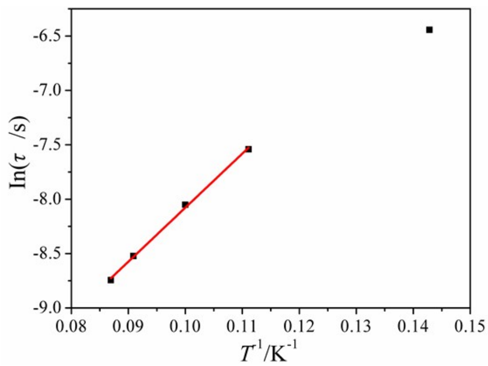

Figure S4. Relaxation time of the magnetization for **1** extracted from the temperature-dependent data under zero-DC field. The red solid lines represent the fitting by the Arrhenius law for high temperature region**.**

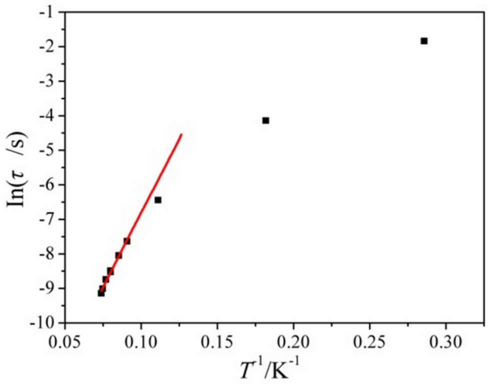

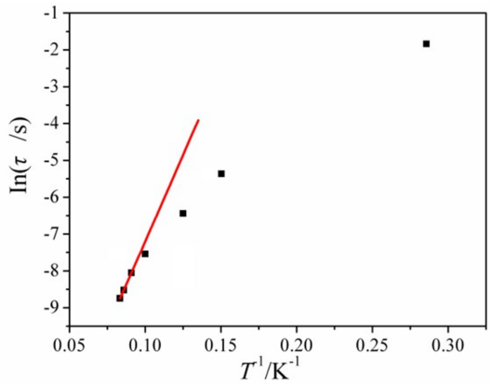

(c) **(d)**

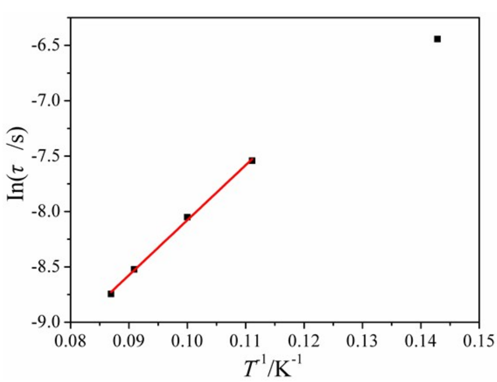

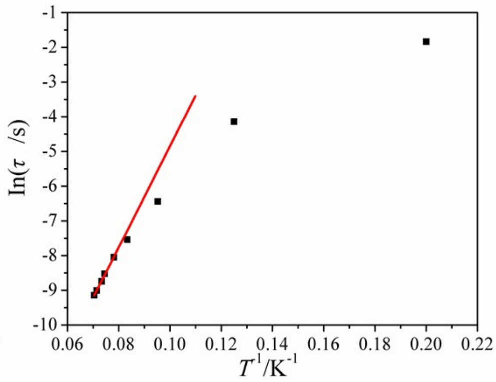

(c) **(d)**

Figure S5. Relaxation time of the magnetization for **1** (a)-**4** (d) extracted from the temperature-dependent data under an applied dc field of 1200 Oe. The red solid lines represent the fitting by the Arrhenius law for high temperature region**.**

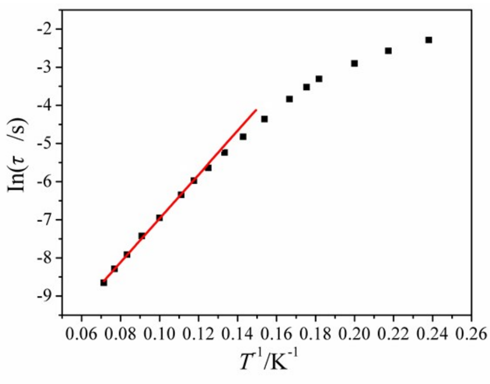

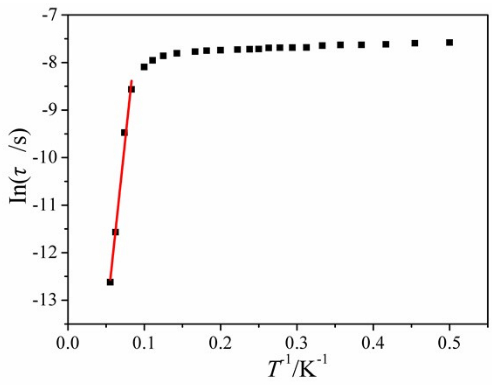

(a) **(b)**

Figure S6. Relaxation time of the magnetization for **3** (a) and **4** (b) extracted from the frequency-dependent data , by fitting the χ''_M vs. frequency curves based on the Debye model, under 1200 Oe-DC field. The red solid lines represent the fitting by the Arrhenius law for high temperature region**.**

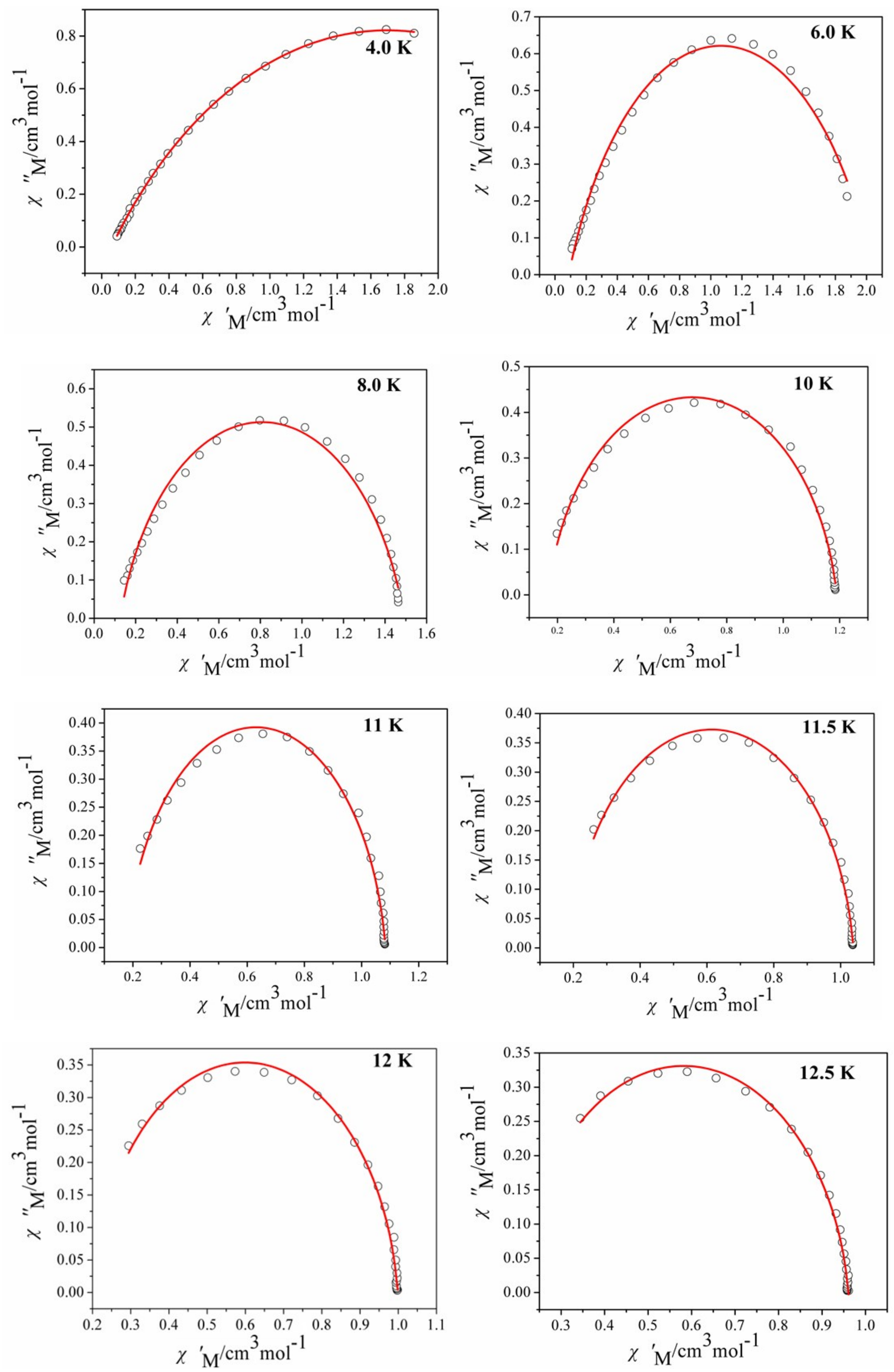
4.0 K
6.0 K
8.0 K
10 K
11 K
11.5 K
12 K
12.5 K
χ ''M/cm3mol-1
χ 'M/cm3mol-1

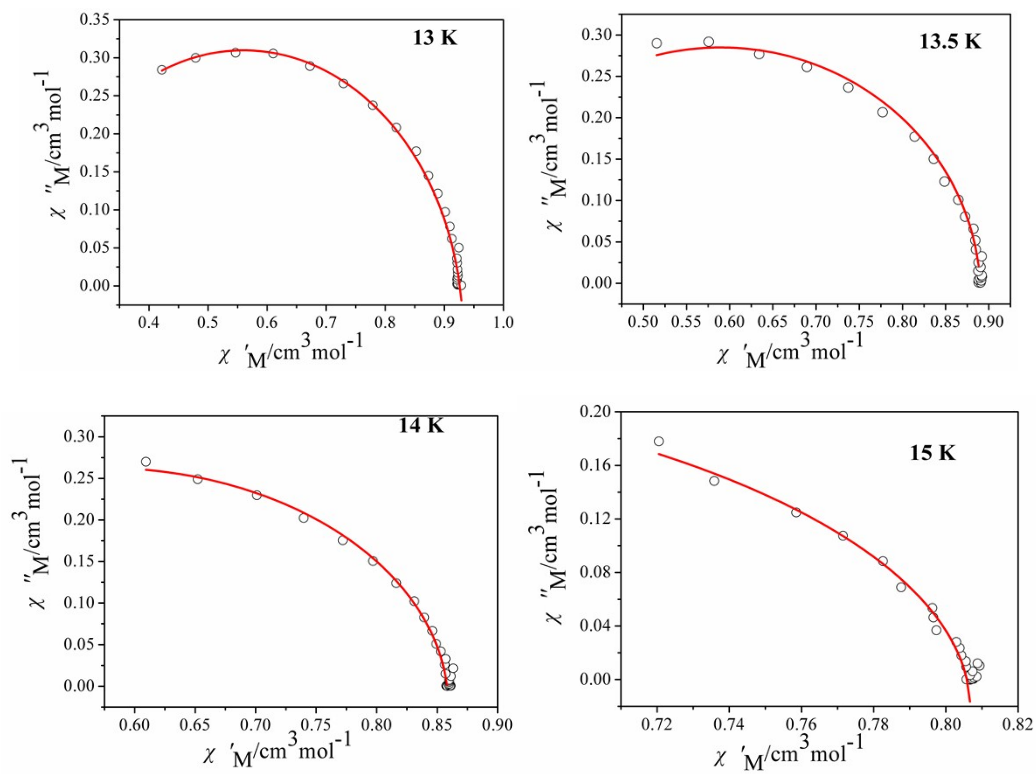

Figure S7. Simulations of dynamical susceptibility $\chi(\omega)$ of **1** ranging from 4 to 15 K in a Cole-Cole diagram. Red lines were performed using the sum of two modified Debye functions with the fitting parameters in Table S4.

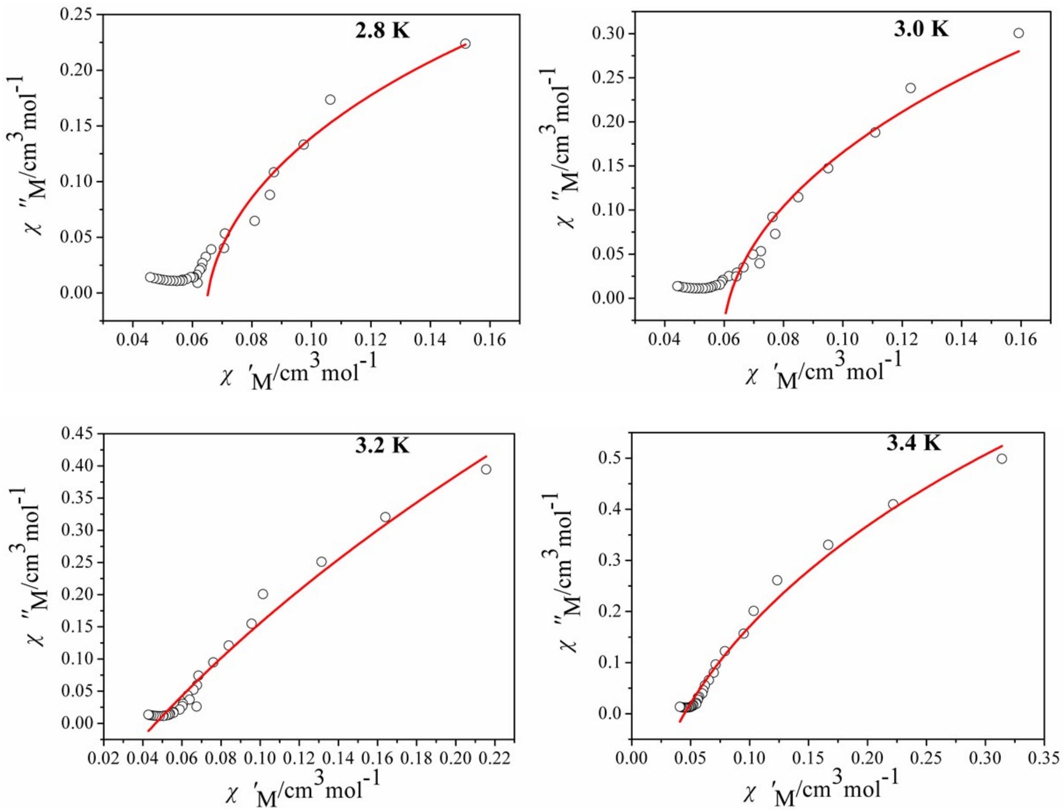

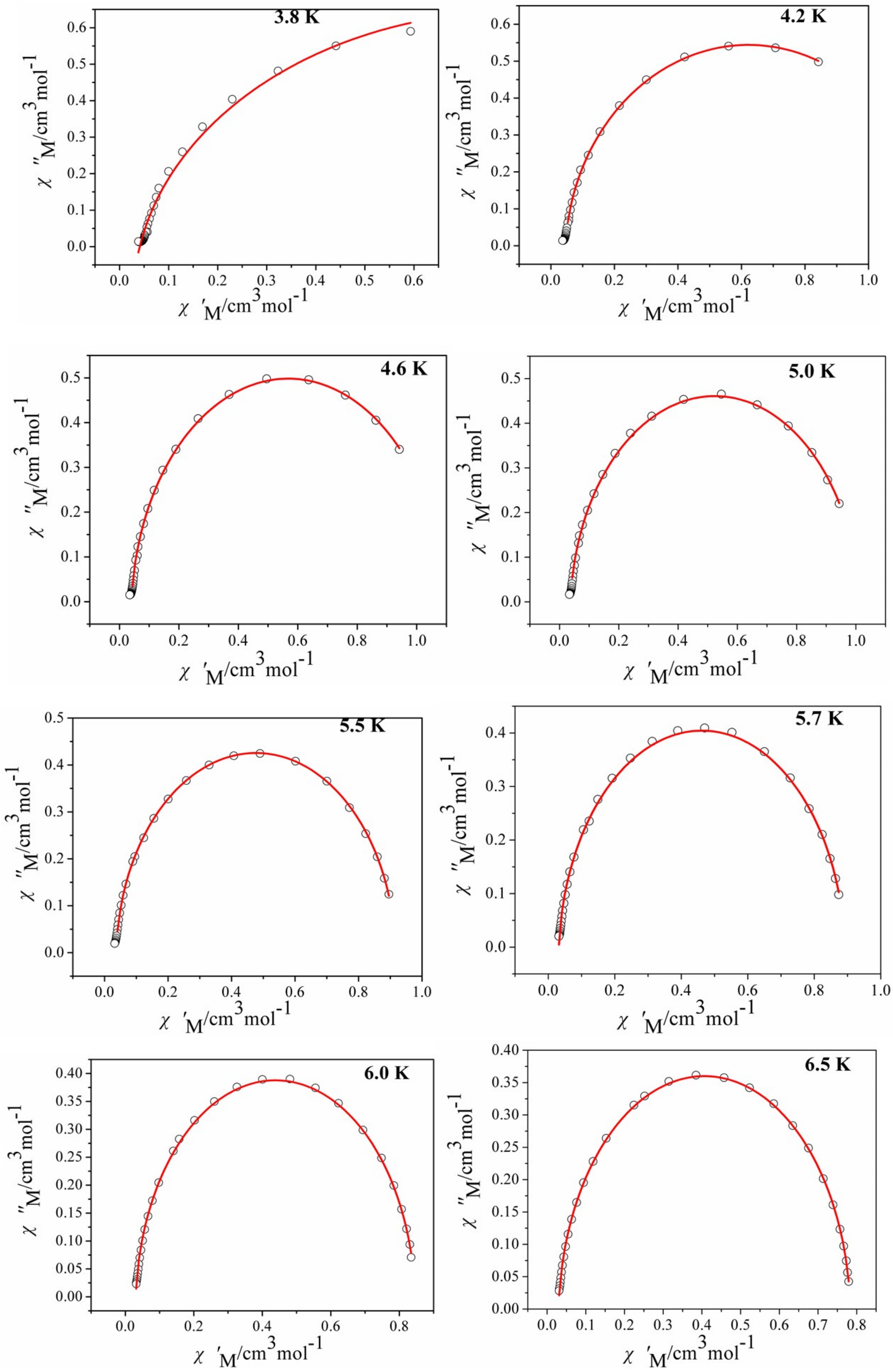
3.8 K
4.2 K
4.6 K
5.0 K
5.5 K
5.7 K
6.0 K
6.5 K
χ ″M/cm3mol-1
χ ′M/cm3mol-1

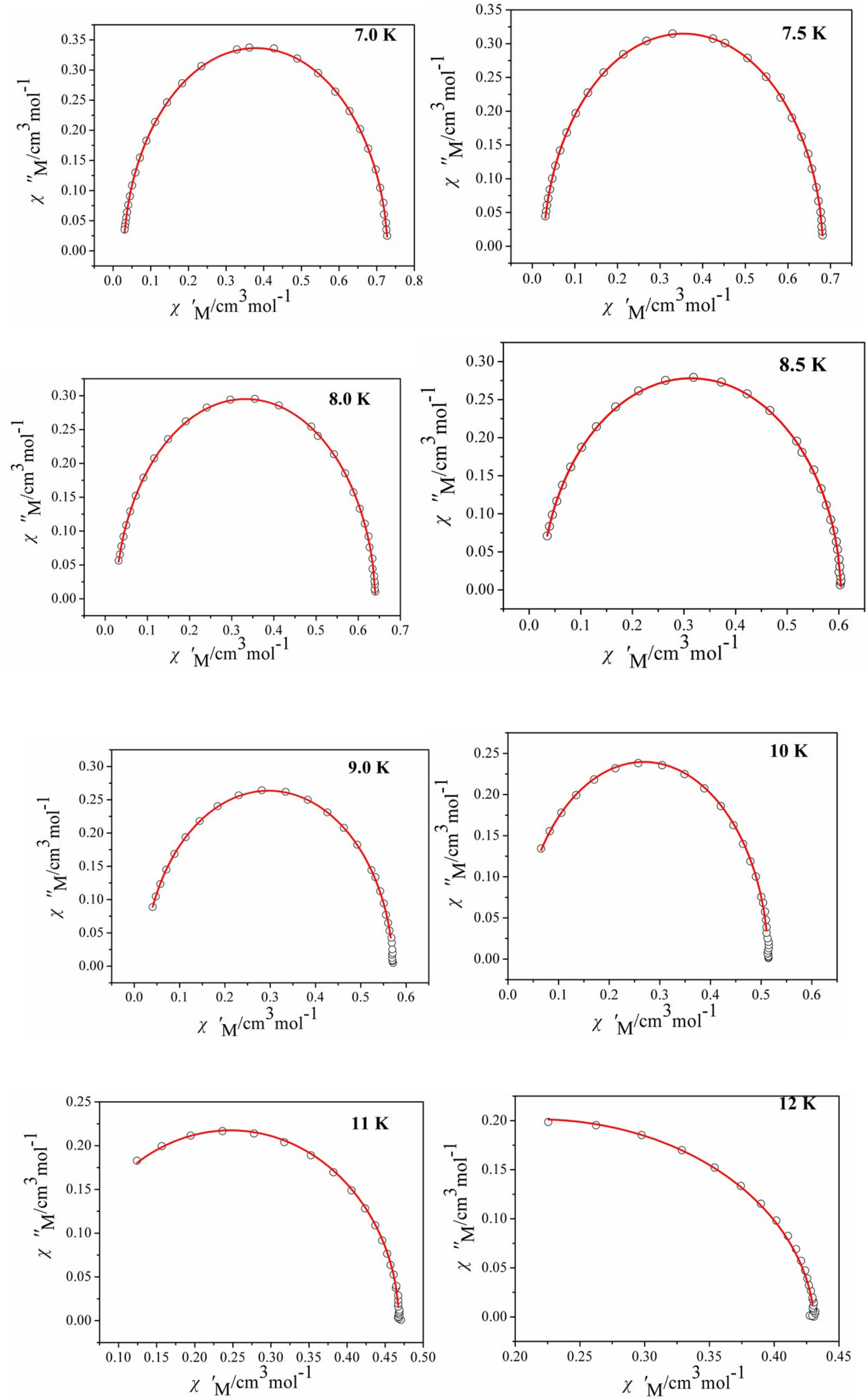
7.0 K
7.5 K
8.0 K
8.5 K
9.0 K
10 K
11 K
12 K
χ ″M/cm3mol-1
χ ′M/cm3mol-1

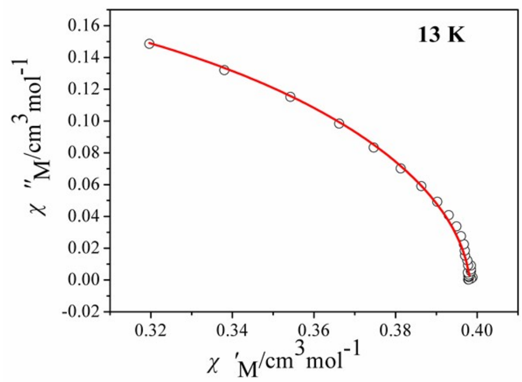

Figure S8. Simulations of dynamical susceptibility $\chi(\omega)$ of **2** ranging from 2.8 to 13 K in a Cole-Cole diagram. Redlines were performed using the sum of two modified Debye functions with the fitting parameters in Table S5.

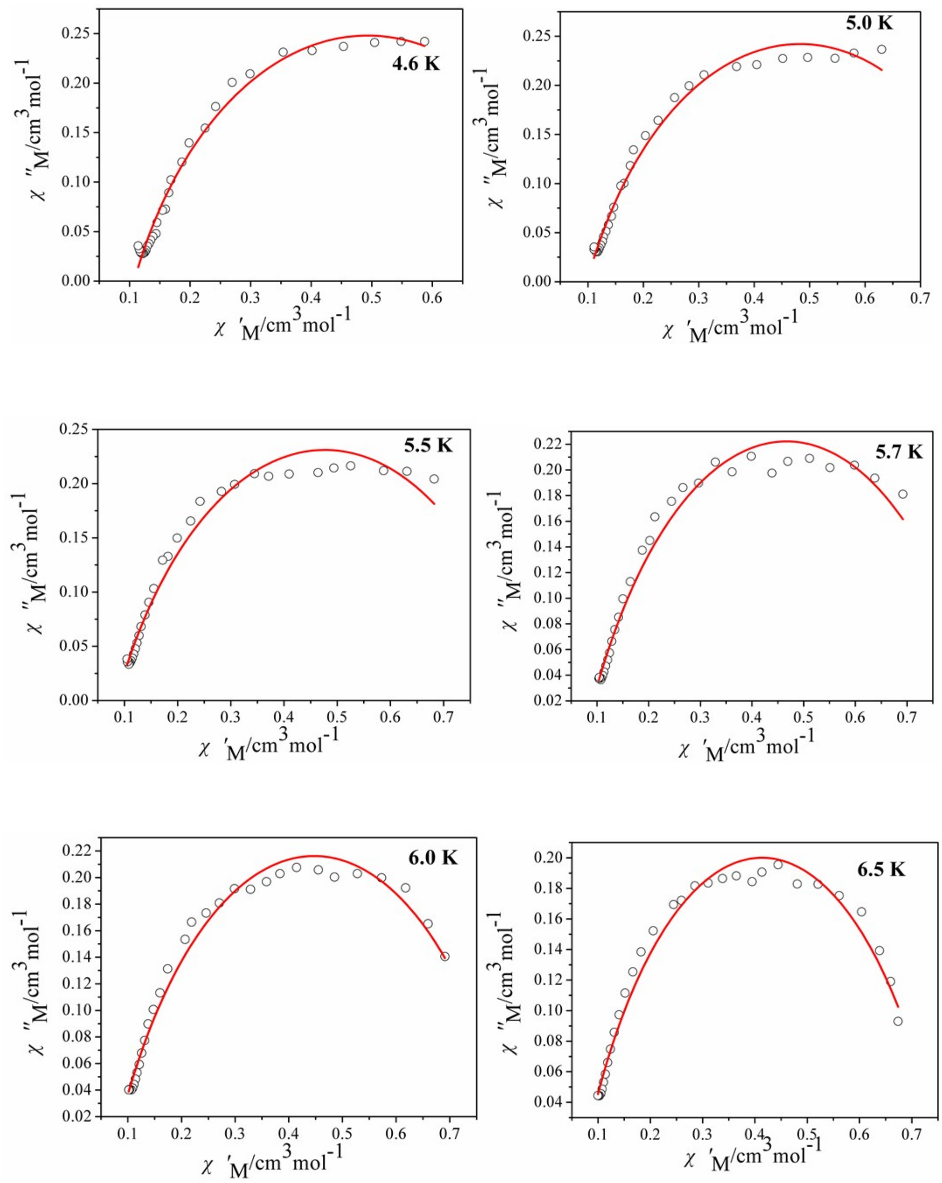

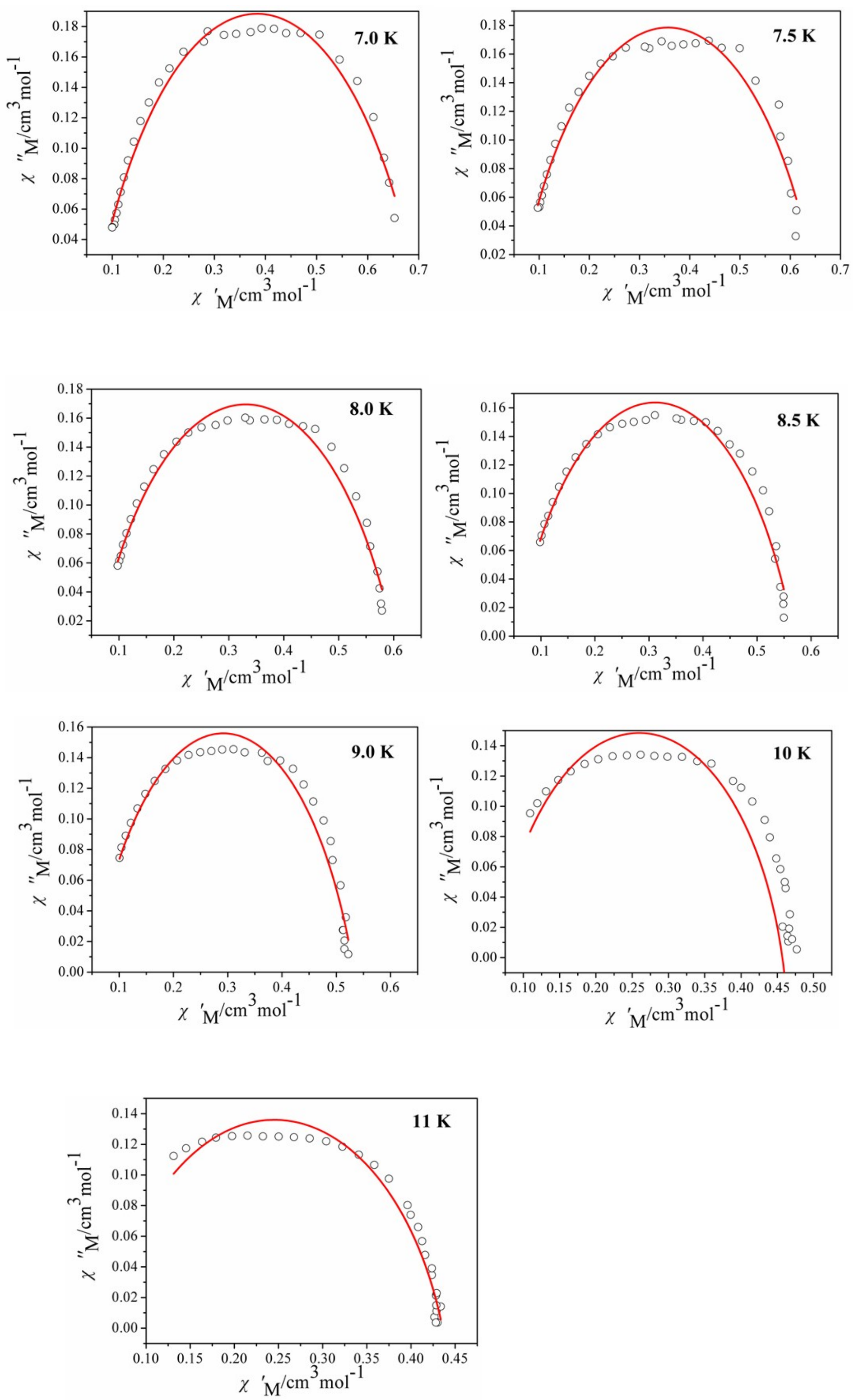

Figure S9. Simulations of dynamical susceptibility $\chi(\omega)$ of **3** ranging from 4.6 to 11 K in a Cole-Cole diagram. Redlines were performed using the sum of two modified Debye functions with the fitting parameters in Table S6.

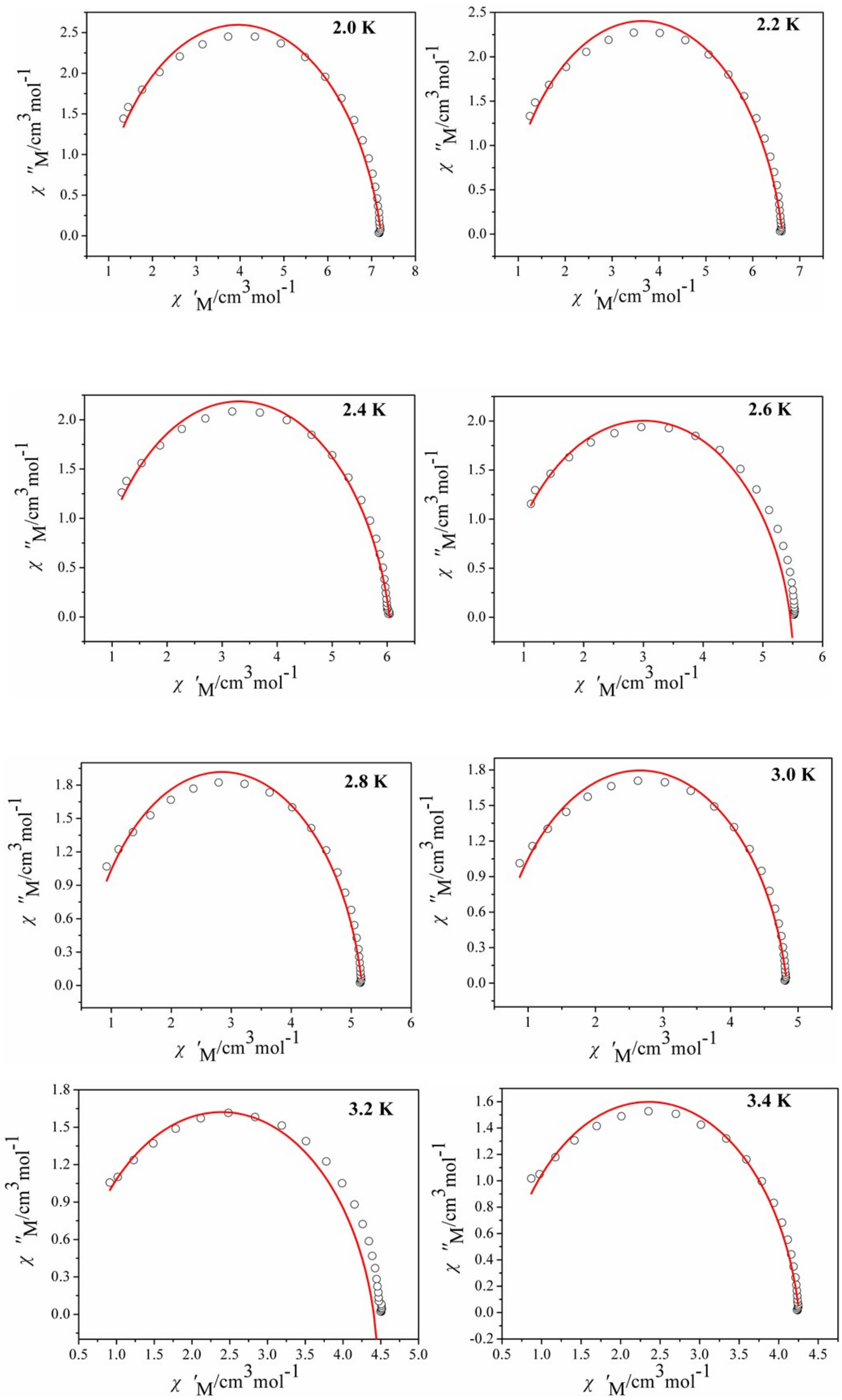
2.0 K
2.2 K
2.4 K
2.6 K
2.8 K
3.0 K
3.2 K
3.4 K
χ "M/cm3mol-1
χ 'M/cm3mol-1

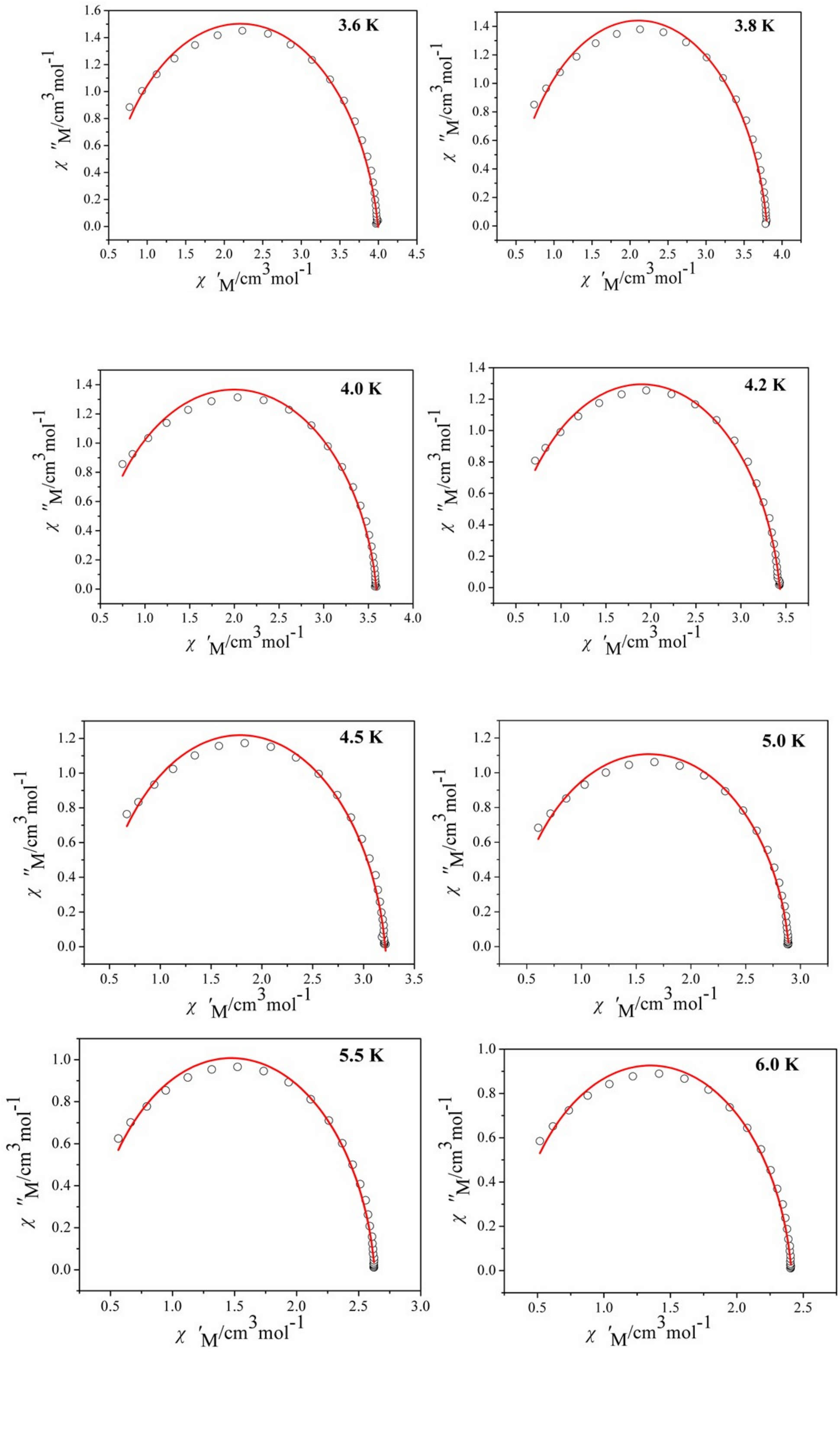
3.6 K
3.8 K
4.0 K
4.2 K
4.5 K
5.0 K
5.5 K
6.0 K
χ ″M/cm3mol-1
χ ′M/cm3mol-1

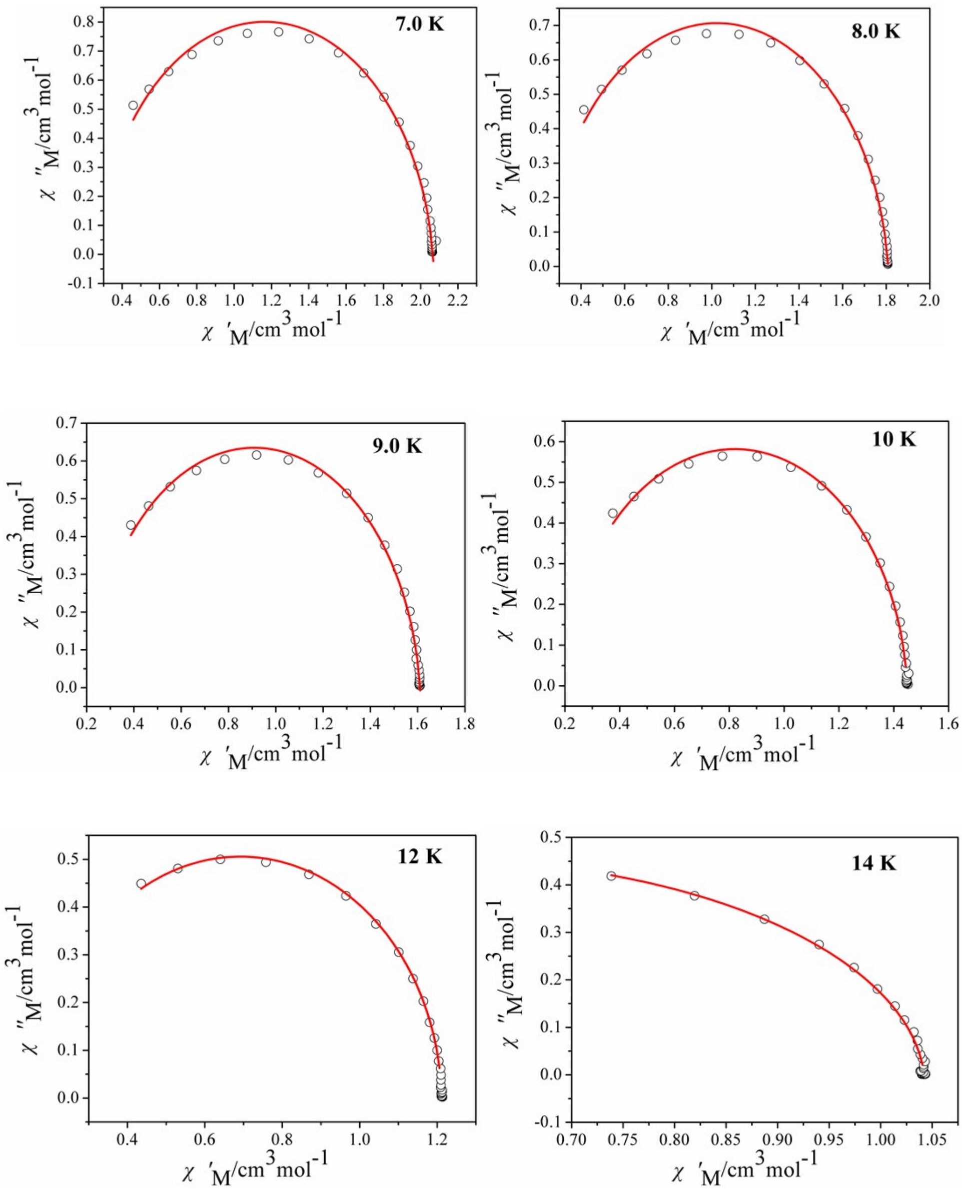

Figure S10. Simulations of dynamical susceptibility $\chi(\omega)$ of **4** ranging from 2.0 to 14 K in a Cole-Cole diagram. Redlines were performed using the sum of two modified Debye functions with the fitting parameters in Table S7.

The magnetic susceptibility data were described by the modified Debye functions:[1]

$$\chi'(\omega) = \chi_S + (\chi_T - \chi_S)\frac{1 + (\omega\tau)^{1-\alpha}\sin(\frac{\pi}{2}\alpha)}{1 + 2(\omega\tau)^{1-\alpha}\sin(\frac{\pi}{2}\alpha) + (\omega\tau)^{(2-2\alpha)}}$$

$$\chi''(\omega) = (\chi_T - \chi_S)\frac{(\omega\tau)^{1-\alpha}\cos(\frac{\pi}{2}\alpha)}{1 + 2(\omega\tau)^{1-\alpha}\sin(\frac{\pi}{2}\alpha) + (\omega\tau)^{(2-2\alpha)}}$$

$$\chi''_{\omega=\tau^{-1}} = (\chi_T - \chi_S)\frac{\cos(\frac{\pi}{2}\alpha)}{2 + 2\sin(\frac{\pi}{2}\alpha)} = \frac{1}{2}(\chi_T - \chi_S)\tan\frac{\pi}{4}(1-\alpha)$$

1. F. Habib, G. Brunet, V. Vieru, I. Korobkov, L. F. Chibotaru, M. Murugesu, J. Am. Chem. Soc. 2013, 135, 13242.

Table S4. Relaxation fitting parameters from Least-Squares Fitting of $\chi(\omega)$ data for **1**.

T(K)	$\Delta\chi_1$ (cm^3mol^{-1})	$\Delta\chi_2$ (cm^3mol^{-1})	α_1
4	3.336	0.059	0.408
6	2.041	0.089	0.278
8	1.492	0.125	0.180
10	1.190	0.167	0.105
10.5	1.134	0.171	0.097
11	1.084	0.177	0.091
11.5	1.038	0.190	0.082
12	0.999	0.199	0.077
12.5	0.961	0.202	0.086
13	0.926	0.194	0.106
13.5	0.890	0.289	0.034
14	0.858	0.285	0.055
15	0.806	0.304	0.053

Table S5. Relaxation fitting parameters from Least-Squares Fitting of $\chi(\omega)$ data for **2**.

T(K)	$\Delta\chi_1$ (cm^3mol^{-1})	$\Delta\chi_2$ (cm^3mol^{-1})	α_1
2.8	4.848	0.065	0.038
3.0	3.256	0.062	0.054
3.2	2.885	0.046	0.190
3.4	2.542	0.045	0.155
3.8	1.588	0.041	0.115
4.2	1.199	0.046	0.037
4.6	1.094	0.041	0.035
5.0	1.011	0.037	0.035
5.5	0.912	0.036	0.022
5.7	0.893	0.032	0.040
6.0	0.846	0.031	0.032
6.5	0.784	0.029	0.029
7.0	0.729	0.028	0.027
7.5	0.682	0.026	0.026
8.0	0.641	0.025	0.028
8.5	0.604	0.023	0.029
9.0	0.571	0.022	0.026
10	0.514	0.023	0.016
11	0.468	0.026	0.011
12	0.430	0.021	0.040
13	0.398	0.021	0.029

Table S6. Relaxation fitting parameters from Least-Squares Fitting of $\chi(\omega)$ data for **3**.

T(K)	$\Delta\chi_1$ (cm^{3}mol^{-1})	$\Delta\chi_2$ (cm^{3}mol^{-1})	α_1
4.6	0.879	0.108	0.272
5.0	0.867	0.099	0.284
5.5	0.869	0.085	0.322
5.7	0.853	0.080	0.336
6.0	0.818	0.077	0.327
6.5	0.757	0.070	0.329
7.0	0.701	0.066	0.319
7.5	0.651	0.062	0.307
8.0	0.603	0.058	0.292
8.5	0.567	0.055	0.275
9.0	0.533	0.051	0.269
10	0.457	0.062	0.179
11	0.436	0.054	0.211

Table S7. Relaxation fitting parameters from Least-Squares Fitting of $\chi(\omega)$ data for **4**.

T(K)	$\Delta\chi_1$ (cm^{3}mol^{-1})	$\Delta\chi_2$ (cm^{3}mol^{-1})	α_1
2.0	7.226	0.686	0.146
2.2	6.634	0.658	0.138
2.4	6.044	0.584	0.140
2.6	5.550	0.556	0.128
2.8	5.182	0.511	0.125
3.0	4.833	0.485	0.121
3.2	4.408	0.377	0.137
3.4	4.257	0.451	0.111
3.6	3.996	0.418	0.110
3.8	3.804	0.417	0.102
4.0	3.591	0.403	0.098
4.2	3.433	0.363	0.108
4.5	3.214	0.357	0.101
5.0	2.894	0.338	0.091
5.5	2.629	0.318	0.089
6.0	2.411	0.289	0.086
7.0	2.065	0.265	0.074
8.0	1.809	0.239	0.067
9.0	1.610	0.209	0.063
10	1.450	0.191	0.050
12	1.212	0.171	0.018
14	1.042	0.084	0.035

(a)

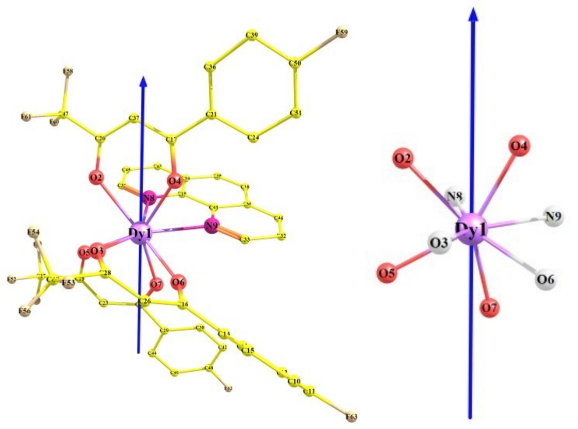

(b)

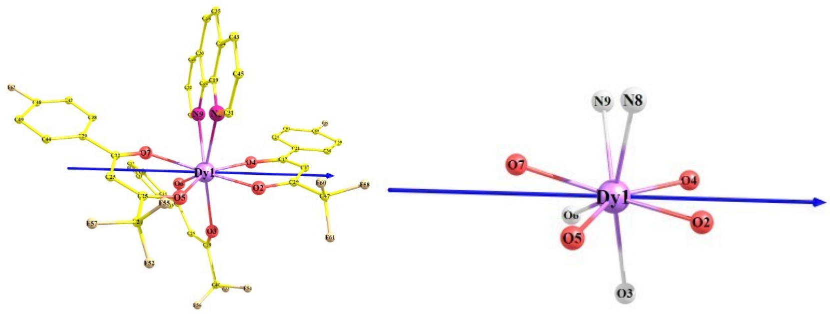

Figure S11. The orientation of the easy axis (g_Z) of the ground KD of **2** obtained from *ab initio* calculations

(a)

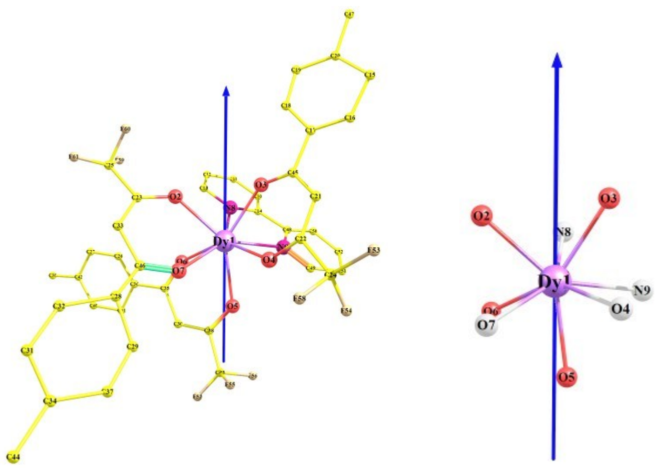

(b)

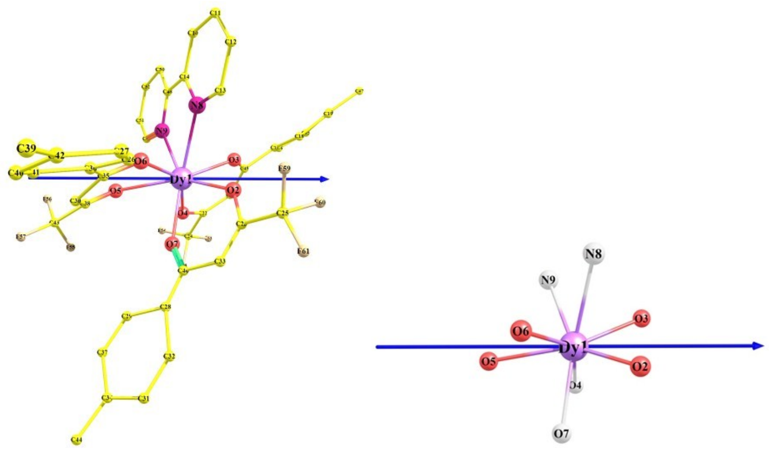

Figure S12. The orientation of the easy axis (g_Z) of the ground KD of **3** obtained from *ab initio* calculations.

(a)

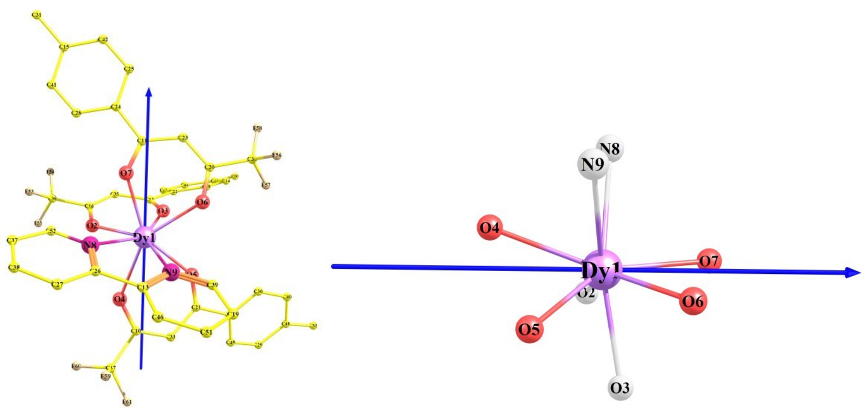

(b)

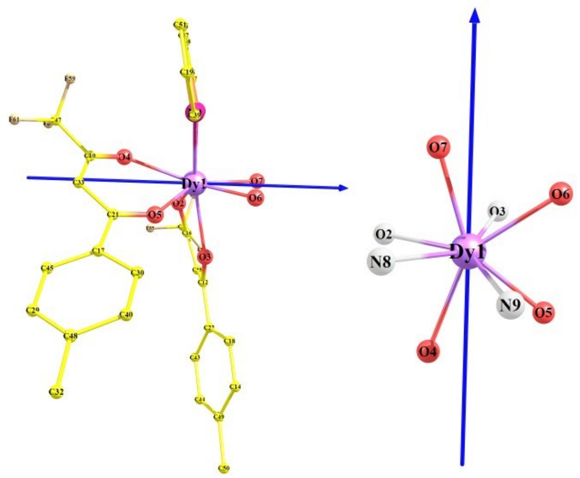

Figure S13. The orientation of the easy axis (g_Z) of the ground KD of **4** obtained from *ab initio* calculations.

Table S8. Decomposition of the wavefunctions of ground KDs of 1-4 into components corresponding to the lowest atomic multiplet J=15/2, | JM >

		Wavefunction composition
1	KD_0-1	**91.57%** $\left\|15/2\right\rangle$ **+7.19%** $\left\|11/2\right\rangle$
	KD_0-2	**91.57%** $\left\|-15/2\right\rangle$ **+7.19%** $\left\|-11/2\right\rangle$
2	KD_1-1	**85.20%** $\left\|-15/2\right\rangle$ **+13.57%** $\left\|-11/2\right\rangle$
	KD_1-2	**85.20%** $\left\|15/2\right\rangle$ **+13.57%** $\left\|11/2\right\rangle$
3	KD_1-1	**78.93%** $\left\|-15/2\right\rangle$ **+1.87%** $\left\|-13/2\right\rangle$ **+11.87%** $\left\|-11/2\right\rangle$ **+2.98%** $\left\|-9/2\right\rangle$ **+2.57%** $\left\|-5/2\right\rangle$
	KD_1-2	**78.93%** $\left\|15/2\right\rangle$ **+1.87%** $\left\|13/2\right\rangle$ **+11.87%** $\left\|11/2\right\rangle$ **+2.98%** $\left\|9/2\right\rangle$ **+2.57%** $\left\|5/2\right\rangle$
4	KD_0-1	**93.88%** $\left\|-15/2\right\rangle$ **+5.53%** $\left\|-11/2\right\rangle$
	KD_0-2	**93.88%** $\left\|15/2\right\rangle$ **+5.53%** $\left\|11/2\right\rangle$

Table S9 Coplanarity of the first-sphere atoms at the equatorial positions for **1-4**

1	O4	O5	N8	N9	average
Z_coordinate	-0.5099	0.2617	-0.3333	0.0729	-0.1272
Deviation from average	-0.3287	0.3889	-0.2061	0.2001	|0.2810|
2	O3	O6	N8	N9	average

Z_coordinate	0.4058	-0.7206	0.1072	-0.1350	-0.0856
Deviation from average	0.4914	-0.6350	0.1928	-0.0494	|0.3422|
3	O4	O7	N8	N9	average
Z_coordinate	0.1245	-0.3376	0.4724	-0.6438	-0.0961
Deviation from average	0.2206	0.1299	0.5685	-0.5477	|0.3667|
4	O2	O3	N8	N9	average
Z_coordinate	0.0003	-0.4184	-0.2432	0.4225	-0.0597
Deviation from average	0.0600	-0.3587	-0.1835	0.4822	|0.2711|